

Supporting Information

Nanowires of Geobacter sulfurreducens require redox cofactors to reduce metals in pore spaces too small for cell passage

Authors: Kyle Michelson^{†,‡}, Robert A. Sanford[§], Albert J. Valocchi[†], Charles J. Werth^{‡,*}

[†]Department of Civil and Environmental Engineering, University of Illinois at Urbana-Champaign, 205 North Mathews Avenue, Urbana, IL 61801.

[‡]Department of Civil, Architectural, and Environmental Engineering, University of Texas at Austin, 301 E. Dean Keeton Street, Austin, TX 78712.

[§]Department of Geology, University of Illinois at Urbana-Champaign, 1301 W. Green St., Urbana, IL 61801.

Contents:

Pages S1-S21

Figures S1-S9

Tables S1-S2

Supporting Information

Materials. All reagents were of ACS reagent grade or cell culture grade, and used without further purification. Solutions were prepared with distilled, deionized water (DDW; 18.2M Ω cm, Millipore Co.) and delivered to the microfluidic reactor in 2.5 mL Hamilton gastight syringes.

Culture Conditions. Growth medium was dispensed into 125 mL serum bottles, sparged with N₂:CO₂ (80:20), and sealed with butyl rubber stoppers before autoclaving. Sodium sulfide was added to bottles at a concentration of 30 μ M to reduce media prior to inoculation. *G. sulfurreducens* was revived from a frozen stock of the same generation and cultured at 24 °C with 8 mM acetate and 3 mM birnessite to verify metal-reducing activity. Cells were then transferred into fresh media with 11 mM acetate and 20 mM fumarate. Once planktonic, cells were infused by syringe into the microfluidic reactor, which was placed inside an environmental chamber set to 24 °C. In one set of experiments, *G. sulfurreducens* was maintained at 31 °C to prevent the formation of nanowires¹. *E. coli* was revived from frozen stock, and cultured at 30 °C in freshwater media supplemented with 5 mM glucose as the sole carbon and energy source. Cells were infused through the microfluidic reactor after being diluted in freshwater medium to 5% of the stock concentration.

All solutions infused through the microfluidic reactor were prepared in the same media with the following modification: The sulfide concentration was decreased from 30 μ M to 5 μ M. Sulfide was added to scavenge oxygen remaining in the gastight syringes after filling. Syringes containing the redox indicator resorufin showed that the reducing potential of 5 μ M sulfide was maintained for less than 2 hours in the absence of *E. coli*. Since syringes were stored overnight to

remove gas bubbles, we did not consider sulfide as an active reductant during infusion. Long-term abiotic controls in the microfluidic reactor showed no reduction of birnessite by sulfide, and experiments with *E. coli* and 5 μ M sulfide in the absence of *G. sulfurreducens* were also negative for birnessite reduction. The combination of 5 μ M sulfide and 0.5 mM glucose allowed for fast reduction, and sustained redox buffering between $-130 \text{ mV} \leq E_p \leq -370 \text{ mV}$ as evidenced by color changes in syringes containing the redox indicators indigo carmine ($E_m^7 = -130 \text{ mV}$) and benzyl viologen ($E_m^7 = -370 \text{ mV}$). Reduced conditions in the reactor were confirmed with resorufin ($E_m^7 = -110 \text{ mV}$) by exploiting the fluorescent properties of the dye in its oxidized state. Redox indicators were only used in preliminary experiments to investigate the effect of redox potential on birnessite reduction.

Batch culture experiments. *G. sulfurreducens* and *E. coli* were grown on birnessite in separate pure cultures and also in co-culture to explore the effect of *E. coli* on birnessite reduction. Pure cultures of *G. sulfurreducens* were grown in 125 mL serum bottles with 3 mM birnessite and 11 mM acetate, while pure cultures of *E. coli* and co-cultures also contained either 0.5 mM or 5 mM glucose. Six replicates were performed for each condition. Additional batch cultures of *G. sulfurreducens* and *E. coli* were used to explore reduction of birnessite at elevated temperature and collect reduced material for analysis by X-ray powder diffraction (XRD). In these experiments, pure cultures and co-cultures were maintained at 31 °C to prevent nanowire formation¹ and explore whether *G. sulfurreducens* is capable of reducing birnessite by direct contact at elevated temperature. Reduced solids from six replicates were poured into 50 mL centrifuge tubes, washed and centrifuged 3 times in DI water, dried at room temperature, and ground into a powder by mortar and pestle for XRD analysis.

Batch Adsorption Experiments.

Sorption of riboflavin to *Geobacter* was evaluated in batch experiments. Briefly, *Geobacter* was grown in replicate 20 mL bottles of media on 5 mM fumarate and 10 mM acetate until biofilms began to form (5-7 days). We then added 5 mM birnessite to the bottles, and upon initial reduction (within 2 days, as indicated by the presence of white rhodochrosite precipitates), aqueous samples were taken and analyzed for background riboflavin. Immediately thereafter, the bottles were spiked with the equivalent of 300 nM riboflavin, mixed for 20 minutes, and then aqueous samples were again taken and analyzed. Control bottles with only media and birnessite were also prepared, spiked with 300 nM riboflavin, shook for 20 minutes, and then analyzed. The background riboflavin concentration in the bottles with *Geobacter* was 93.5 ± 1.2 nM, but in the controls it was not detected. After spiking with 300 nM riboflavin, the riboflavin concentration was 341 ± 0.6 nM in bottles with *Geobacter*, and 287 ± 0.6 nM in the controls. The decrease in the bottles with *Geobacter* from 380.5 nM (i.e., $287+93.5$) to 341 ± 0.6 nM indicates sorption occurred, and the larger decrease for the bottles with *Geobacter* compared to the bottles with only birnessite indicate sorption was to cell material. To further probe the sorption mechanism, the bottles with *Geobacter* were incubated an additional day, and then samples were taken for riboflavin analysis. Immediately thereafter, the bottles were spiked with 1 U/g of a serine protease (i.e., Savinase) and sampled for analysis. Serine protease digests outer membrane cytochromes without killing or lysing the cells²; this is expected to release bound riboflavin due to conformational changes induced in the cytochromes. We measured 226 ± 2 nM in the bottles before Savinase addition, and 355 ± 4 nM after Savinase addition, indicating that riboflavin was sorbed to *Geobacter* cytochromes. The Savinase had no effect on riboflavin concentration in the control bottles with only media and birnessite.

Microfluidic Reactor Fabrication. Microfluidic reactors were etched in silicon using a combination of photolithography and electron beam lithography (EBL). A schematic illustrating the major steps of fabrication is shown in Figure S2. ZEP520A electron beam resist was spin coated on a silicon wafer, and a digitized image of a nanoporous wall was transferred into the resist using a JEOL-6000 FSE EBL system (JEOL Ltd., Japan). Microfluidic channels were etched using photolithography to a depth of 10 μm using inductively coupled plasma - deep reactive ion etching (ICP-DRIE) on a Plasma-Therm Versaline DSE (Plasma-Therm LLC, USA). The nanoporous wall was 1 cm long and consisted of an alternating series of pillars and gaps. After etching, the pillars measured 1.0 x 1.0 μm in area and gaps were 0.6 μm wide. Nanopores were closed by depositing a uniform layer of polysilicon on the wafer by low pressure chemical vapor deposition (LPCVD), resulting in Pillars were 1.4 x 1.4 μm in area while the gaps (i.e. nanopores) were $\leq 0.2 \mu\text{m}$ wide. Two inflow and two outflow ports approximately 1 mm in diameter were ultrasonically drilled. The reactors were encapsulated by anodically bonding the silicon wafers to Borofloat 33 glass wafers at 900 V and 400 °C. Once bonded, PEEK NanoPort assemblies (IDEX Corporation, Illinois, USA) were glued over the drilled ports and connected to 0.01" ID PEEK tubing. PEEK and ETFE fittings connected the tubing to gastight syringes that were driven by a NE-4002X microfluidic syringe pump (New Era Pump Systems Inc., New York, USA).

Cleaning and sterilization. Biofilm, birnessite, and rhodochrosite in microfluidic reactors left over from previous experiments were removed by successive infusions of 0.3 M HNO₃, 20% (v/v) serine protease $\geq 16 \text{ U/g}$, 1% (w/v) sodium dodecyl sulfate, and 75% isopropyl alcohol. NanoPorts were detached and reactors were briefly soaked in boiling Piranha solution containing 2:1 (v/v) concentrated sulfuric acid and 30% H₂O₂ to remove glue from the surface. Reactors

were then sterilized by autoclaving and reassembled in a biological safety cabinet. These steps were also performed on newly fabricated reactors to ensure similar surface chemistry between experiments. Solutions prepared for infusion were kept sterile by autoclaving gastight syringes before filling, autoclaving chemical stocks with the exception of riboflavin and AQDS, and performing all critical work in a biological safety cabinet. Riboflavin and AQDS were sterilized by filtration through sterile 0.22 μm syringe filters.

Raman Spectroscopy. Mineralogical analyses were performed in-situ on a Horiba LabRAM HR Evolution confocal Raman system (HORIBA Scientific, Kyoto, Japan). Raman spectra were taken between 0 and 1200 cm^{-1} using a 532 nm DPSS laser in a backscattering configuration. The laser was calibrated daily using silicon as a reference material, and reference spectra from the RUFF mineral database were used to identify minerals inside the reactor. Birnessite spectra were obtained at 5 mW and averaged over 3 successive scans with an acquisition time of 60 seconds. Rhodochrosite spectra were obtained at 2.5 mW and averaged over 15 successive scans with an acquisition time of 10 seconds.

Light Microscopy. Brightfield and fluorescence images were taken on a Nikon Eclipse TI-E (Nikon, Kobe, Japan) inverted microscope integrated with the Raman system. Autofluorescence of cytochrome C was detected by exciting *G. sulfurreducens* cells within a range of 340-380 nm and filtering emission between 435-485 nm through a 400 nm dichroic mirror. The dead cell stain propidium iodide and the redox dye resorufin were excited between 540-580 nm, and fluorescence was detected through a 595 nm dichroic mirror and 600-660 nm emission filter. The live cell stain Syto-9 was excited between 457-487 nm, and fluorescence was detected through a

495 nm dichroic mirror and 502-538 nm emission filter. Fluorescent images were taken with a Andor Zyla 5.5 camera and color images with a Lumenera Infinity 3-1UR camera.

HPLC Analyses. Effluent was analyzed every 24 hours by reversed-phase high performance liquid chromatography (HPLC) for riboflavin, flavin mononucleotide (FMN), and flavin adenine dinucleotide (FAD) using a Shimadzu LC-2040C HPLC, and Shimadzu C18 reversed-phase column (50 mm x 2.1 mm with 1.9 μm particle size). Separation was achieved at 45 °C with an isocratic concentration of 30% methanol versus an aqueous solution of acetic acid at pH 4.7, for 3.5 minutes, at a flow rate of 0.2 mL/min. A Shimadzu RF-20 fluorescence detector was used with an excitation wavelength of 450 nm and an excitation wavelength of 520 nm, and peak area was calculated using LabSolutions Lite LC/GC software, Ver. 5.82.

XRD Analyses. XRD patterns were collected at room temperature in transmission mode on a Rigaku R-Axis Spider diffractometer (Rigaku, Tokyo, Japan) with an image plate detector using a graphite monochromator with CuK α radiation ($\lambda = 1.5418\text{\AA}$). The R-Axis Spider was operated using Rigaku's RINT Rapid Version 2.3.8 diffractometer control program. The powder sample was mounted on a Hampton Research CryoLoop. The 2-dimensional image plate data was converted to a conventional 1-dimensional powder pattern using Rigaku's 2DP Version 1.0 data conversion program. The data were analyzed using Bruker Analytical's DiffracPLUS Evaluation Package, EVA (V. 2009).

TEM Analyses. Bright field transmission electron microscope (TEM) images were taken on a JEOL 2010f operated at 200kV with a Gatan OneView camera.

Estimation of Riboflavin Concentration in the Nanoporous Wall. In the absence of added riboflavin (i.e., only endogenously produced riboflavin), the concentration of riboflavin in the effluent of the microfluidic reactor could be lower than in the nanopores because of dilution from the influent flow, assuming that riboflavin production is occurring mainly in the *Geobacter* biofilm and not by planktonic *E. coli* cells. However, since the time scale of diffusion across a channel ($t = L^2/D = (0.0250 \text{ cm})^2/(4 \times 10^{-6} \text{ cm}^2/\text{sec}) = 156 \text{ sec}$) is on the order of the fluid retention time in the reactor ($t = 60 \text{ sec}$), we assumed these concentrations would be quite close. To more rigorously evaluate this assumption, we identified a steady state two-dimensional analytical solution provided by Seagren et al. (1994), which assumes advection of clean fluid over a surface which is at a constant concentration, and the following governing equation and boundary conditions³:

$$v_x \frac{\partial C}{\partial x} = D_z \frac{\partial}{\partial z} \left(\frac{\partial C}{\partial z} \right) \quad (1)$$

$$C(x, z = \infty) = 0 \quad (\text{semi} - \text{infinite domain}) \quad (2)$$

$$C(x, z = 0) = C_s \quad \text{for } 0 \leq x \leq L_x \quad (3)$$

$$C(x = 0, z) = 0 \quad (4)$$

where v_x (0.017 cm/sec) is the velocity of water flowing parallel to the biofilm surface, C is the riboflavin concentration at any location at or above the biofilm surface along the entire length of the nanoporous wall, x is the longitudinal distance along the wall, L_x (1 cm) is the length of the wall, z is the distance away from the biofilm surface into the flow channel, and D_z ($4 \times 10^{-6} \text{ cm}^2/\text{sec}$) is the riboflavin diffusion coefficient. The analytical solution to the above governing equation and boundary conditions is:

$$F_{avg} \left[\frac{M}{t} \right] = 2v_x C_s A \sqrt{\frac{D_z}{v_x L_x \pi}} \quad (5)$$

where F_{avg} represents the mass averaged flux from biofilm at the biofilm-water interface, which is equal to the flux of riboflavin in the effluent from one channel of the reactor, i.e., $F_{avg} = F_{effluent}$, and A (0.001 cm x 1 cm) is the biofilm area at the biofilm-water interface. The value of $F_{effluent}$ can be calculated from the water flow rate in a channel, Q , and the measured riboflavin effluent concentration, $C_{effluent}$, as follows:

$$F_{avg} = F_{effluent} = QC_{effluent} = 1.25 \times 10^{-7} \text{ nmol/min} \quad (6)$$

Solving for C_s in Equation 5, we obtain 7 nM. This is only slightly greater than the measured value of 5 nM measured in the reactor effluent. Therefore, the concentration of riboflavin in the nanoporous wall is likely only slightly more than 5 nM, and much less than the 100 nM added to the reactor to stimulate birnessite reduction across the wall.

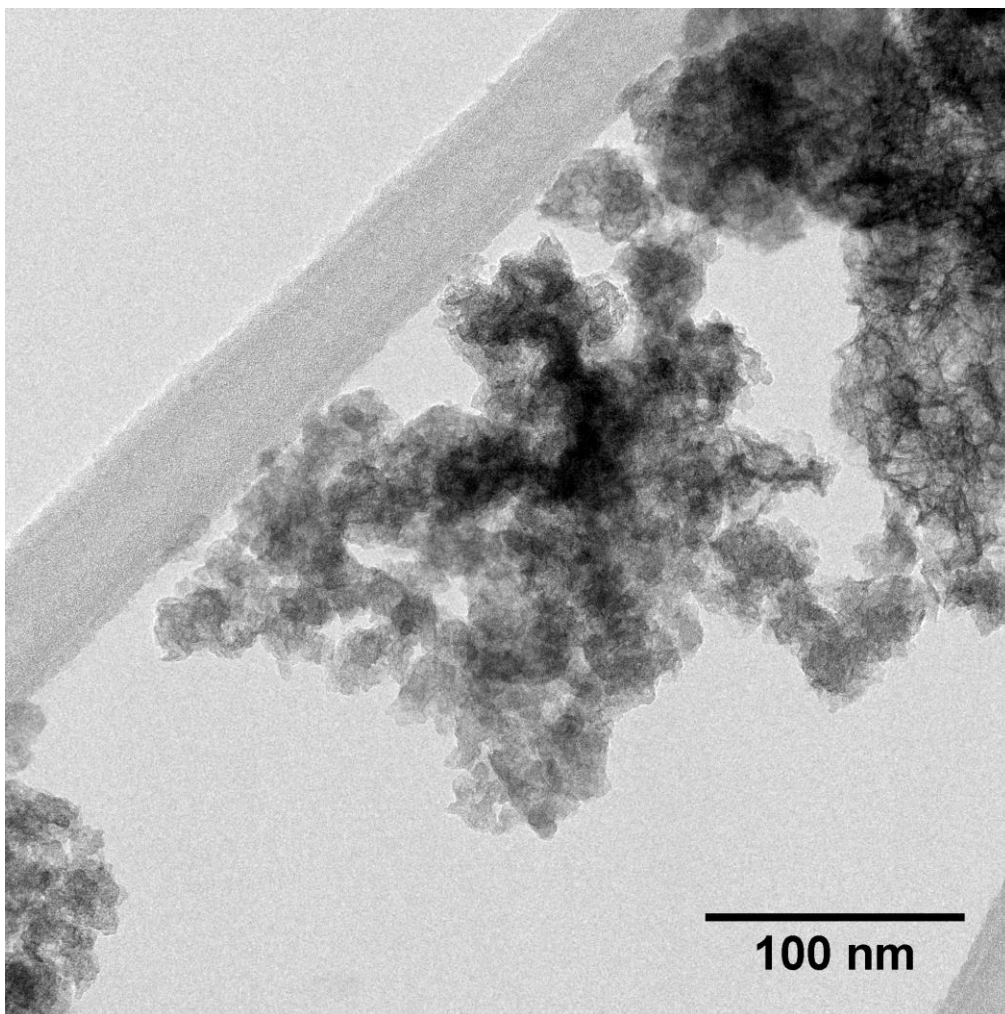


Figure S1. TEM image of dried birnessite particles with individual crystals < 100 nm.

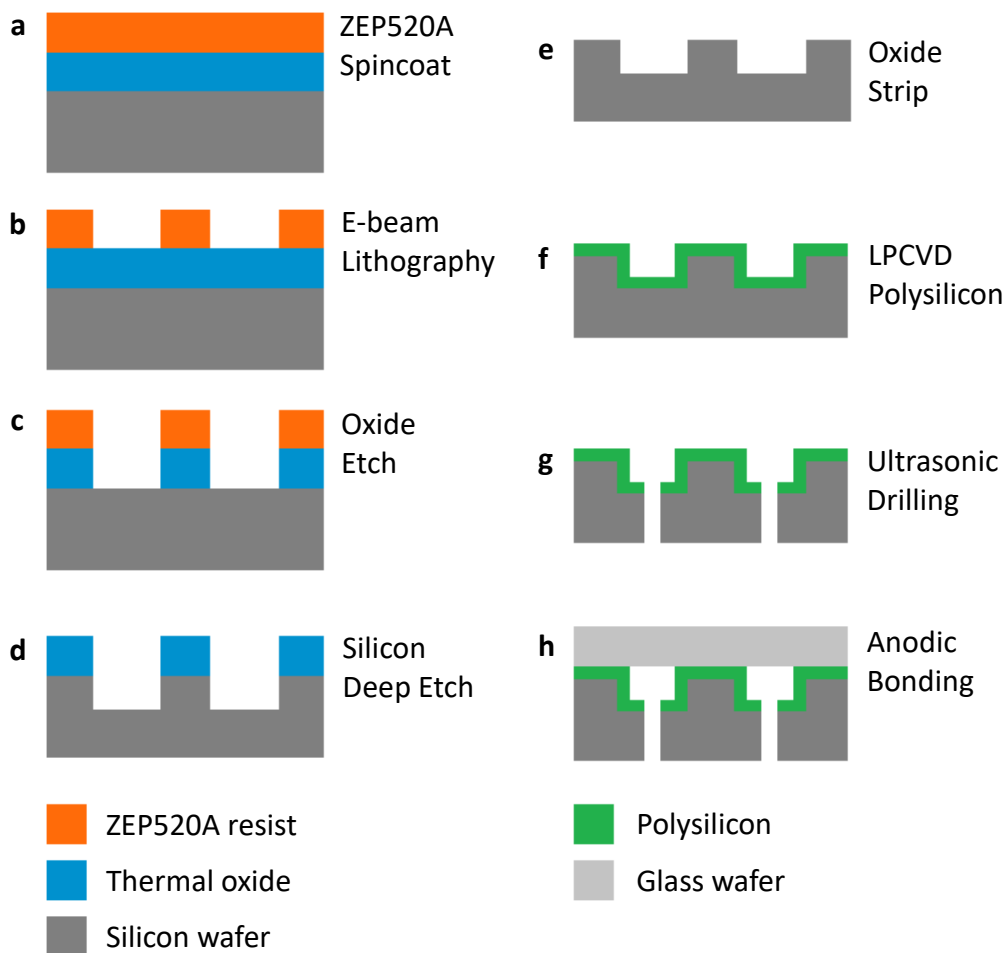


Figure S2. Process diagram for reactor fabrication. **(a)** spincoating of ZEP520A e-beam resist **(b)** E-beam patterning of wall and channels **(c)** CF_4 plasma etch of exposed oxide **(d)** silicon deep etch to 10 microns **(e)** stripping of remaining oxide by BOE **(f)** LPCVD of polysilicon to close the gap between pillars to <200 nm **(g)** ultrasonic drilling of ports and **(h)** anodic bonding of silicon wafer to glass.



Figure S3. Fluorescent image of reactor taken during infusion of resorufin with or without *E. coli*, with arrows indicating flow direction and dashed lines showing the boundary of the channel opposite the nanoporous wall.

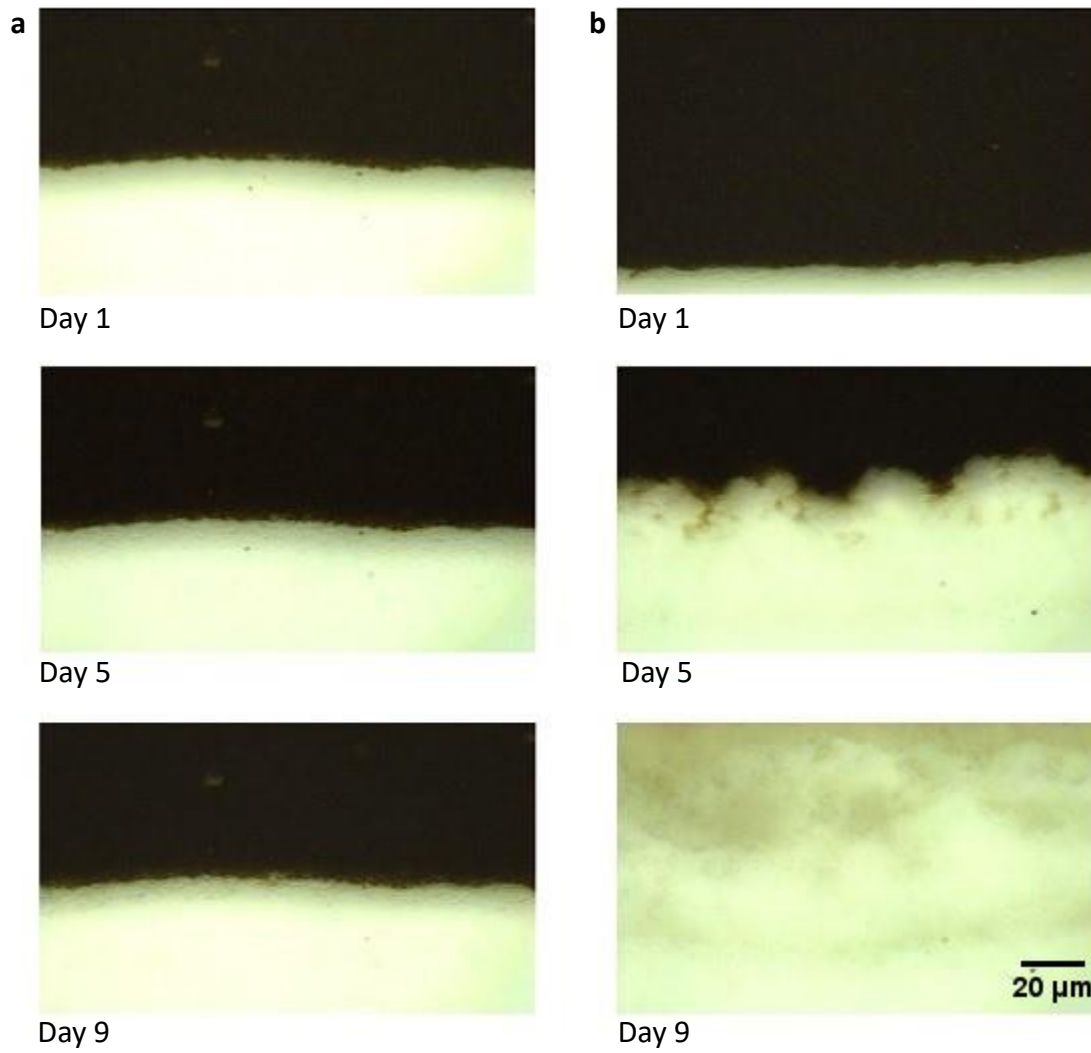


Figure S4. Influence of *E. coli* on birnessite reduction by direct cell contact. (a) No reduction is observed with *G. sulfurreducens* in pure culture. (b) Birnessite is fully reduced after 9 days with the addition of *E. coli* in co-culture.

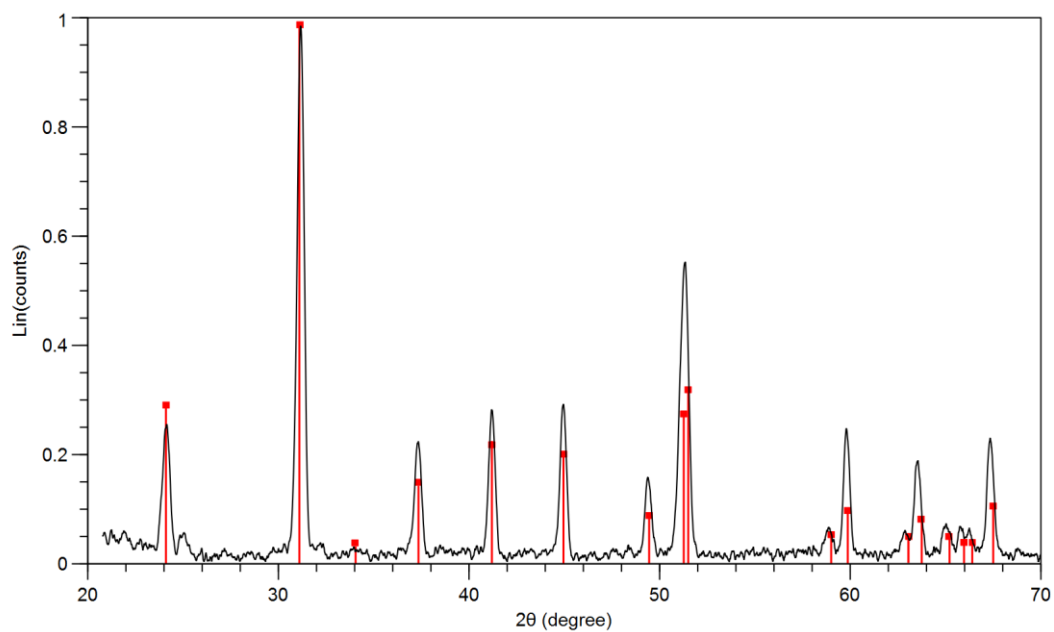


Figure S5. X-ray powder diffraction pattern of precipitates collected from several batch experiments following birnessite reduction. Reference data for rhodochrosite are shown in red.

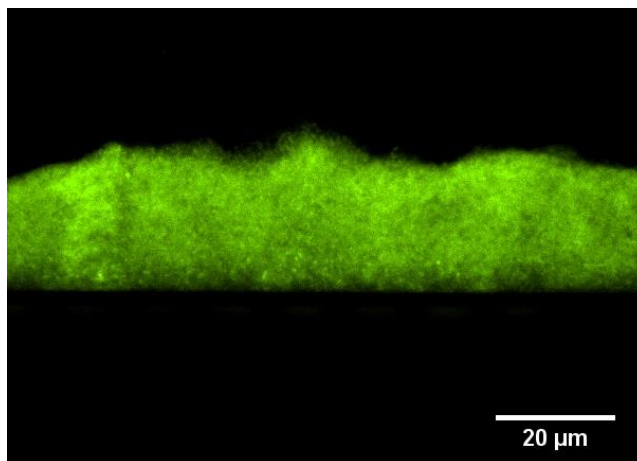


Figure S6. Metabolic staining of biofilm with RedoxSensor Green during LR-EET of birnessite.

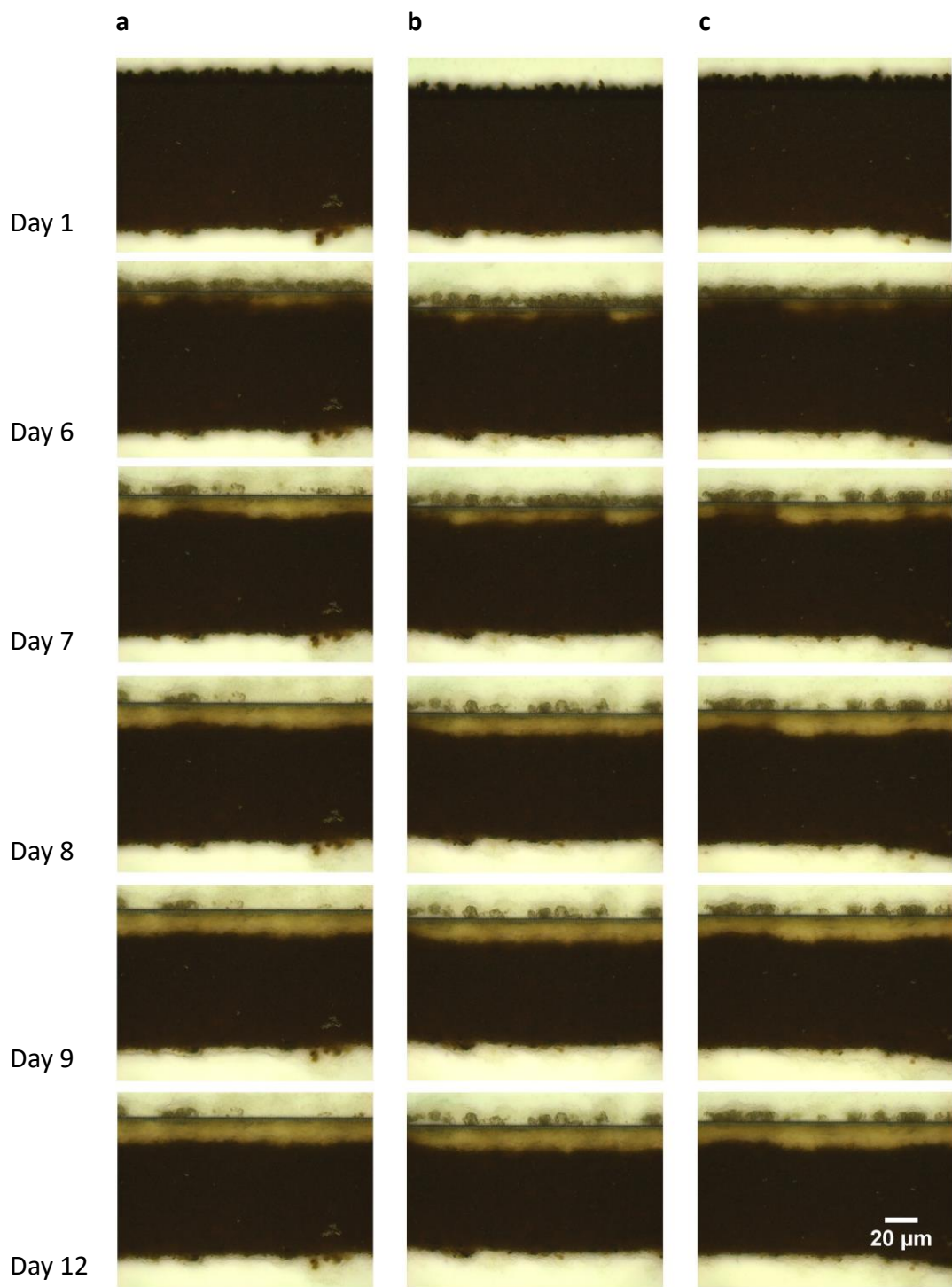


Figure S7. Time lapse images of birnessite reduction observed upstream (a), center (b), and (c) downstream in the reactor.

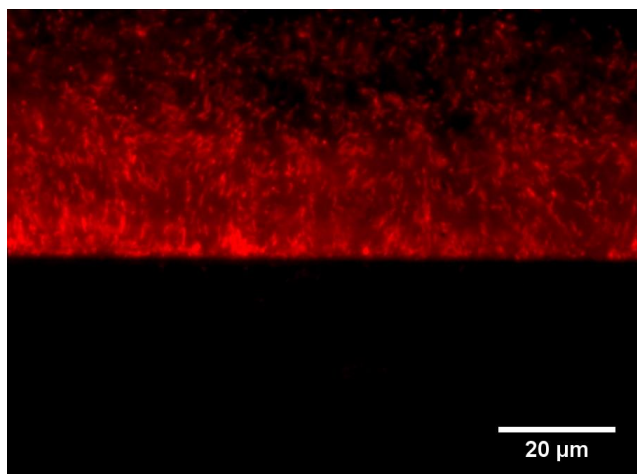
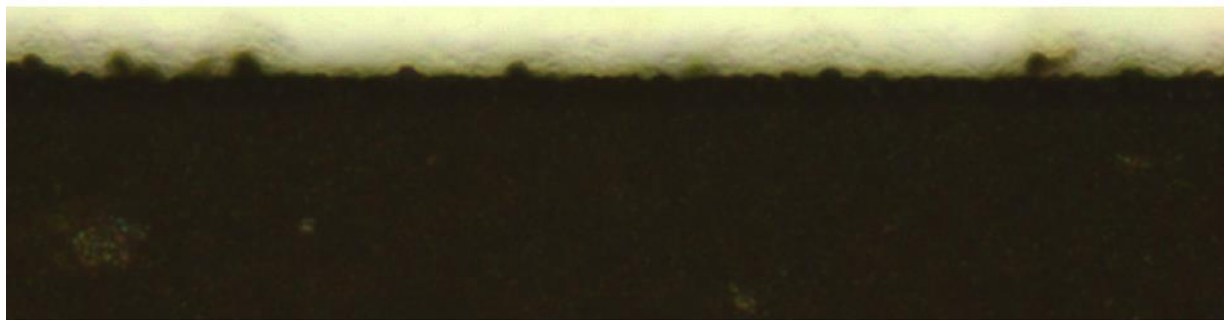
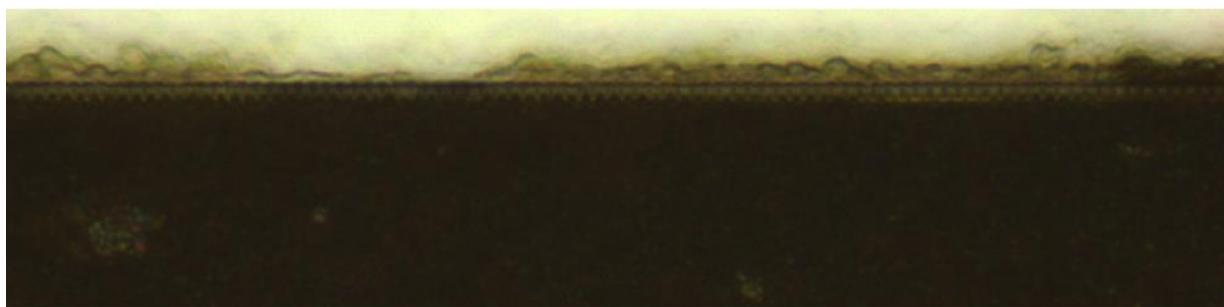


Figure S8. Dead cell staining with propidium iodide after inactivation by glutaraldehyde. Note the absence of cells below the nanoporous wall at the centerline.

Day 1



Day 4



Day 9

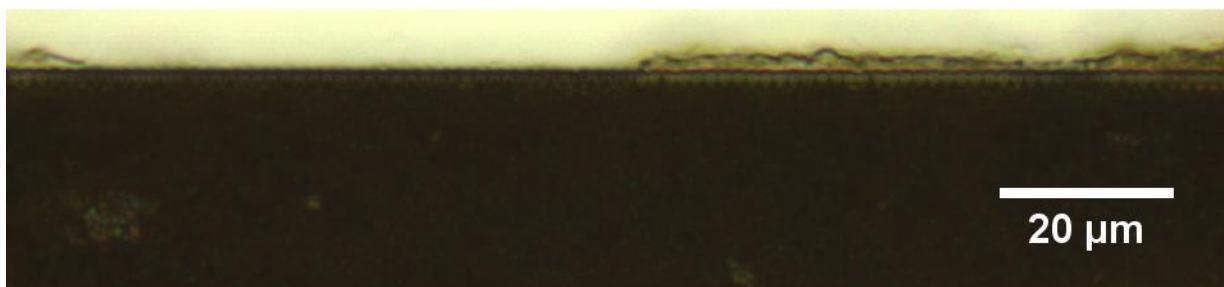


Figure S9. Progression of birnessite reduction by *G. sulfurreducens* KN400 grown at $31\text{ }^{\circ}\text{C} \pm 1\text{ }^{\circ}\text{C}$, showing reduction of birnessite by direct contact, but not by LR-EET.

Table S1. Experimental set-up and flow conditions

Stage	Inlet	Component	Flow Rate (nL/min)
1	Top + Bottom	Sterilize flow channels	250
2	Top + Bottom	Purge flow channels with media	250
3	Bottom	Immobilize birnessite in bottom flow channel	Manual
4	Top	Inoculate <i>G. sulfurreducens</i> in top flow channel	125
	Bottom	Infuse 1 mM fumarate in bottom flow channel	125
5	Top + Bottom	Infuse <i>E. coli</i> + 0.5 mM glucose + 10 mM acetate + riboflavin / AQDS	50

Table S2. Summary of conditions and results for batch culture experiments

Observation	-----Conditions-----				-----Results-----
	G. sulfurreducens KN400	E. coli K-12	Temp. (°C)	RF / AQDS [†]	Days required to reduce Mn
No reduction by media components*	X	X	24, 31	X,✓	X
No reduction by E. coli*	X	✓	24, 31	X,✓	X
Reduction by G. sulfurreducens	✓	X	24	X,✓	8-10
Reduction stimulated by E. coli	✓	✓	24	X,✓	5-6
Activity increased at 31 °C	✓	X	31	X,✓	6-8
Reduction by concentrated lysate	X	✓	24	X	21-30

* Control experiments, X not present or observed, ✓ present or observed

[†] Experiments performed with riboflavin or AQDS, or neither

References

- (1) Cologgi, D. L.; Lampa-Pastirk, S.; Speers, A. M.; Kelly, S. D.; Reguera, G. Extracellular reduction of uranium via *Geobacter* conductive pili as a protective cellular mechanism. *Proc. Natl. Acad. Sci. U. S. A.* **2011**, *108*, 15248–15252.
- (2) Qian, X.; Reguera, G.; Mester, T.; Lovley, D. R. Evidence that OmcB and OmpB of *Geobacter sulfurreducens* are outer membrane surface proteins. *FEMS Microbiol. Lett.* **2007**, *277* (1), 21–27.
- (3) Seagren, E. A.; Rittmann, B. E.; Valocchi, A. J. Quantitative Evaluation of the Enhancement of NAPL-Pool Dissolution by Flushing and Biodegradation. *Environ. Sci. Technol.* **1994**, *28* (5), 833–839.